

Supporting Information

Highly Efficient, NiAu-catalyzed Hydrogenolysis of Lignin into Phenolic Chemicals

Jianguang Zhang, Hiroyuki Asakura, Jeaphianne van Rijn, Jun Yang, Paul Duchesne, Bin Zhang, Xi Chen, Peng Zhang, Mark Saeys* and Ning Yan*

Contents

1 Materials	3
2 Synthesis of substrates	3
2.1 Organosolv Lignin.....	3
2.2 2-phenoxy-1-phenethanol	3
2.3 2-(2-methoxyphenyl)oxy-1-phenethanol.....	4
2.4 2-(2,6-dimethoxyphenyl)oxy-1-phenethanol.....	4
2.5 1-benzyloxy-2-methoxybenzene	4
3 Catalyst preparation and reaction	4
3.1 Catalyst preparation.....	4
3.2 Hydrogenolysis reaction.....	5
3.3 Product identification	5
3.4 Determination of the amount of active sites by CS ₂ poisoning	11
4 Catalyst characterization.....	12
4.1 Transmission electron microscopy (TEM).....	12
4.2 X-Ray powder diffraction (XRD)	14
4.3 X-ray photoelectron spectroscopy (XPS)	14
4.4 X-ray absorption (XAS)	14
4.5 UV-vis spectroscopy	15
4.6 Inductively coupled plasma mass spectrometry (ICP-MS).....	16
4.7 DFT calculation.....	16
5 Conversion of other lignin model compounds and organosolve lignin	18
5.1 Conversion of organosolv lignin.....	19
5.2 Gel permeation chromatography (GPC)	19

Tables & Figures

Table S1. Catalysts screening on the hydrogenolysis reaction of 2-phenoxy-1-phenethanol.....	7
Table S2. Hydrogenolysis of 2-phenoxy-1-phenethanol over NiAu catalyst with various Ni: Au ratio. ..	8
Table S3. Hydrogenolysis of 2-phenoxy-1-phenethanol over Ni ₇ Au ₃ catalyst as a function of H ₂ pressure.	9
Table S4. Kinetics study on the hydrogenolysis of 2-phenoxy-1-phenethanol over Ni and Ni ₇ Au ₃ catalyst.	9
Table S5. Influence of additives (phenol, toluene, cyclohexanol) on the hydrogenolysis of 2-phenoxy- 1-phenethanol over Ni and Ni ₇ Au ₃ catalyst.	10
Fig. S1. Yield of 2-methoxyphenol as a function of CS ₂ /Metal ratio over a) Ni catalysts and b) Ni ₇ Au ₃ catalysts.	11
Table S6. β-O-4 model compound hydrogenolysis results in literatures.....	11
Fig. S2. TEM images of CO passivated a) Ni, b) Au and c) Ni ₇ Au ₃ catalysts.....	12
Fig. S3. a-i) HAADF-STEM images of Ni ₇ Au ₃ catalysts with five randomly selected catalyst particles, and b) d) f) h) and j) are the EDX spectra of these selected particles.	13
Table S7. Fitting parameters regarding the Fourier-Transformation (FT) and EXAFS fitted regions of Ni ₇ Au ₃ catalyst.....	14
Fig. S4. EXAFS fitting curves for Ni ₇ Au ₃ catalyst at a) Ni K edge and b) Au L _{III} edge.....	15
Table S8. EXAFS fitting results of the Ni ₇ Au ₃ catalyst.	15
Fig. S5. <i>In situ</i> UV-vis monitoring of the formation process of a) Au, b) Ni and c) Ni ₇ Au ₃ catalysts.	16
Fig. S6. Transition states and activation barriers for the hydrogenation of ArO* intermediates on Ni(111) and on Ni ₃ Au(111).	17
Table S9: Relative energies for the overall reaction $XO^* + \frac{1}{2} H_2 (g) \rightarrow XOH + *$ on Ni and NiAu in kJ/mol, as well as the O-H distance of the forming bond in the TS in Å.	17
Fig. S7. Hydrogenolysis of 2-(2-methoxyphenyl)oxy-1-phenethanol and 2-(2,6-dimethoxyphenyl)oxy- 1-phenethanol.	18
Table S10. Hydrogenolysis of 1-benzyloxy-2-methoxybenzene over Ni and Ni ₇ Au ₃ catalyst.	18
Table S11. Hydrogenolysis of diphenyl ether over Ni ₇ Au ₃ catalyst.....	19
Fig. S8. GPC spectra of Organosolv lignin, lignin130 and lignin170	19
Fig. S9. ¹³ C-NMR spectra of a) organosolv lignin, b) products after depolymerization over Ni ₇ Au ₃ at 130 °C and 1 hour (lignin130) and c) products after depolymerization at 170 °C and 12 hours (lignin170).	20

1 Materials

Sodium borohydride (95.0%) was purchased from TCI; polyvinylpyrrolidone (PVP, M.W. = 40000) ammonia perrhenate(VII) and rhodium(III) chloride hydrate (Rh 38.5%-45.5%) were from Alfa Aesar; Fe(II) chloride tetrahydrate (98%), tin(II) chloride dihydrate, 2-bromoacetophenone, potassium carbonate, phenol and guaiacol were from Sigma Aldrich; palladium(II) chloride (Pd 59.50%) and iridium(III) chloride hydrate were from Shaanxi Kaida Chemical Engineering Co., Ltd.; auric chloride acid (Au 50%), chloroplatinic acid (Pt 47%), cobalt(II) chloride hexahydrate (99.0%), nickel(II) chloride hydrate (98.0%), copper(II) chloride (99%) and ruthenium(III) chloride hydrate (Ru 37%) were from Sinopharm Chemical Reagent (SCR). H₂ (99.995%) was from Singapore Oxygen Air Liquide Pte Ltd. (SOXAL). All chemicals were used as received.

2 Synthesis of substrates

NMR spectra were recorded over a Bruker 300 MHz and a Bruker 400 MHz instrument.

2.1 Organosolv Lignin

Organosolv lignin was prepared according to a procedure described in the literature.¹ Birch (*Betula platyphylla* Suk) sawdust (10 g) was extracted with a toluene and ethanol mixture (volume ratio 2:1) for 24 h in a Soxhlet extractor. After drying in the air, the sawdust was placed in a flask with a dioxane and deionized water mixture (volume ratio 9:1) containing HCl (0.7% (w)). After extracting at 90-95 °C for 6 h, the extractor was removed and the solid residue was washed with fresh dioxane. The combined solution was neutralized by NaHCO₃ and then concentrated under reduced pressure to get a viscous black liquid, into which dioxane (10 mL) was added. This mixture was drop-wise added to a Na₂SO₄ aqueous solution (1000 mL, 1% (w)), slowly stirred for 1 h, and then filtrated. The solid was washed with water until no SO₄²⁻ could be detected by Ba(NO₃)₂, and finally dried under vacuum at 60 °C overnight to obtain the organosolv lignin (~1.0 g).

2.2 2-phenoxy-1-phenethanol

The synthetic procedure was based on a modified literature report.² A round bottom flask equipped with a reflux condenser was charged with 2-bromoacetophenone (10.0 g, 50.2 mmol), potassium carbonate (12.3 g, 89.1 mmol), phenol (5.90 g, 62.7 mmol) and acetone (250 mL). The resulting suspension was stirred and heated to reflux overnight, after which it was filtered through Celite and concentrated in vacuo. The resulting solid was crystallized from ethanol to give 2-phenoxy-acetophenone as white crystals (5.9 g, 53%). In a second step, a round bottom flask was charged with 2-phenoxy-acetophenone (5.0 g, 22.5 mmol), tetrahydrofuran (100 mL), and water (25 mL). Sodium borohydride (1.7 g, 45.0 mmol) was added portion-wise to maintain a gentle evolution of gas over 10 minutes, after which the reaction mixture was stirred for 3 h at room temperature. The reaction was quenched with 2 M HCl (5 mL) and then the reaction mixture was diluted with water (50 mL). The aqueous portion was extracted with diethyl ether (3 × 50 mL). The combined organic extracts were washed twice with saturated aqueous NaHCO₃ and dried in vacuo to give of 2-phenoxy-1-phenethanol as a white solid (3.50 g, 69%).¹H NMR (300 MHz, CDCl₃) δ 7.49 (d, *J* = 7.4 Hz, 2H), 7.42 (t, *J* = 7.4 Hz, 2H), 7.36 (t, *J* = 7.2 Hz,

1H), 7.32 (t, $J = 7.5$ Hz, 2H), 7.00 (t, $J = 7.3$ Hz, 1H), 6.95 (d, $J = 8.0$ Hz, 2H), 5.16 (d, $J = 8.9$ Hz, 1H), 4.14 (dd, $J = 9.6, 3.1$ Hz, 1H), 4.04 (t, $J = 9.3$ Hz, 1H), 2.81 (d, $J = 2.4$ Hz, 1H). ^{13}C NMR (75 MHz, CDCl_3) δ 158.4, 139.7, 129.6, 128.6, 128.2, 126.3, 121.3, 114.7, 73.3, 72.6.

2.3 2-(2-methoxyphenyl)oxy-1-phenethanol

Using the procedure described for 2-phenoxy-1-phenethanol, 2-(2-methoxyphenyl)oxy-acetophenone was prepared from 2-bromoacetophenone (5.9 g, 29.7 mmol) and guaiacol (4.1 mL, 37.1 mmol) as a white crystal (3.5 g, 49%). Following that, 2-(2-methoxyphenyl)oxy-1-phenethanol was prepared from 2-(2-methoxyphenyl)oxy-acetophenone (3.5 g, 14.4 mmol) as a white amorphous solid (2.0 g, 57%). ^1H NMR (300 MHz, CDCl_3) δ 7.48 (d, $J = 7.3$ Hz, 2H), 7.41 (t, $J = 7.4$ Hz, 2H), 7.35 (t, $J = 7.3$ Hz, 1H), 7.06 - 7.02 (m, 1H), 6.99 - 6.90 (m, 3H), 5.16 (d, $J = 9.3$ Hz, 1H), 4.22 (dd, $J = 10.1, 2.9$ Hz, 1H), 4.03 (t, $J = 9.7$ Hz, 1H), 3.91 (s, 3H), 3.70 (d, $J = 1.7$ Hz, 1H); ^{13}C (75 MHz, CDCl_3) δ 150.2, 148.0, 139.6, 128.5, 128.0, 126.3, 122.6, 121.1, 116.1, 112.1, 76.3, 72.4, 55.9.

2.4 2-(2,6-dimethoxyphenyl)oxy-1-phenethanol

A round bottom flask equipped with a reflux condenser was charged with 2-bromoacetophenone (9.8 g, 49.2 mmol), potassium carbonate (12.3 g, 89.1 mmol), 2,6-dimethoxyphenol (10.0 g, 50.4 mmol) and acetone (250 mL). The resulting suspension was stirred and heated to reflux overnight, after which it was filtered through Celite and concentrated in vacuo. The resulting liquid raw product was purified over LC by using ethyl acetate:hexane = 1:5 as eluent. Then the product was reduced by sodium borohydride using the procedure described for 2-phenoxy-1-phenethanol to give 2-(2,6-dimethoxyphenyl)oxy-1-phenethanol as a white amorphous solid. ^1H NMR (300 MHz, CDCl_3) δ 7.45 (d, $J = 7.3$ Hz, 2H), 7.39 (t, $J = 7.4$ Hz, 2H), 7.32 (t, $J = 7.2$ Hz, 1H), 7.09 (t, $J = 8.4$ Hz, 1H), 6.67 (d, $J = 8.4$ Hz, 2H), 5.02 (d, $J = 9.9$ Hz, 1H), 4.61 (d, $J = 1.4$ Hz, 1H), 4.48 (dd, $J = 10.9, 2.7$ Hz, 1H), 3.93 (s, 6H), 3.79 (dd, $J = 10.0, 10.8$ Hz, 1H); ^{13}C NMR (75 MHz, CDCl_3) δ 153.3, 139.5, 136.8, 128.4, 127.7, 126.4, 124.2, 105.2, 80.1, 72.5, 56.1.

2.5 1-benzyloxy-2-methoxybenzene

A round bottom flask equipped with a reflux condenser was charged with benzyl bromide (5.95 mL, 50 mmol), potassium carbonate (12.3g, 89.1 mmol), guaiacol (5.58 mL, 50 mmol) and acetone (250 mL). The resulting suspension was stirred and heated to reflux overnight, after which it was filtered through Celite and concentrated in vacuo. The resulting solid was recrystallized from ethanol to give 1-benzyloxy-2-methoxybenzene as white crystals (8.6 g, 80%).

3 Catalyst preparation and reaction

3.1 Catalyst preparation

The following precursors were used as received: $\text{RuCl}_3 \cdot n\text{H}_2\text{O}$, $\text{RhCl}_3 \cdot n\text{H}_2\text{O}$, H_2PtCl_4 , HAuCl_4 , AgNO_3 , CuCl_2 , $\text{FeCl}_2 \cdot 4\text{H}_2\text{O}$, $\text{CoCl}_2 \cdot 6\text{H}_2\text{O}$, $\text{NiCl}_2 \cdot 6\text{H}_2\text{O}$, NH_4ReO_4 and $\text{SnCl}_2 \cdot 2\text{H}_2\text{O}$. For catalysts containing Pd and Ir, PdCl_2 and $\text{IrCl}_3 \cdot n\text{H}_2\text{O}$ were first transformed into H_2PdCl_4 and HIrCl_4 , respectively, by adding

stoichiometric amount of HCl. All catalysts containing Ni employed NiCl₂·6H₂O as the precursor, except for NiAg that used Ni(NO₃)₂·6H₂O to prevent the formation of AgCl.

Desired amount of precursors (metal content: 0.044 mmol) and PVP (97.6 mg, 0.88 mmol) were dissolved in water (4 mL) and charged into a 25 ml flask with a magnetic stirrer. Then NaBH₄ (8.3 mg, 0.22 mmol) was dissolved in water (2 mL) and was added quickly under vigorous stirring (1000 rpm) at room temperature (25 °C). As a sign of reduction, the mixture would turn to dark brown/black color in 1~30 seconds, depending on different precursors. The stirring was stopped at 30 seconds and the catalyst solution was immediately transferred into an autoclave for catalytic reactions, or freeze-dried for analysis. Note: over-exposure to air will significantly decrease the activity of the catalysts containing Ni, due to oxidation!

3.2 Hydrogenolysis reaction

In a typical experiment, the substrate (0.22 mmol), fresh catalyst (0.022 mmol in 3 mL water) and magnetic stirrer were charged into a high pressure reactor (20 mL). After flushing with H₂ three times, the reactor was charged with 10 bar H₂, and put into a preheated oil bath with a stirring speed of 1000 rpm. After the reaction, the reactor was quenched to ambient temperature using cooling water, and the organic products were extracted using ethyl acetate (6mL) and analyzed by gas chromatography (GC) and GC-mass spectroscopy (GC-MS) on an Agilent 7890A gas chromatograph with flame ionization detector (FID) and an Agilent 7890A-5975 GC-MS instrument, both equipped with HP-5 capillary columns (30 m × 250 μm). The peak area was calibrated by FID effective carbon number (ECN) of the representing compound. Conversion is defined as the amount of rings in products divided by divided by the total amount of rings found on GC-FID, multiplied by 100%; the yield is defined as the amount of rings divided by the total amount of rings found on GC-FID, multiplied by 100%:

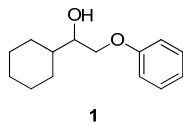
$$Conversion(\%) = \left(1 - \frac{2 \times Area_{sub}/ECN_{sub}}{\sum(Area_i/ECN_i) + 2 \times \sum(Area_j/ECN_j) + 2 \times Area_{sub}/ECN_{sub}} \right) \times 100\%$$

$$Yield_x(\%) = \frac{n \times Area_x/ECN_x}{\sum(Area_i/ECN_i) + 2 \times \sum(Area_j/ECN_j) + 2 \times Area_{sub}/ECN_{sub}} \times 100\%$$

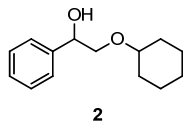
Where n is the number of ring(s) in molecule, e.g., n = 1 for monomers, and n = 2 for dimers; i is subscript for monomers, while j is subscript for dimers.

3.3 Product identification

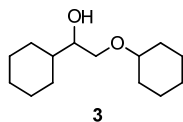
Hydrogenolysis products **4-15** were identified by GC-MS and further confirmed by comparison with authentic samples. To identify products **1-3**, the reaction was scaled up ten times employing Pt as catalyst (since Pt gives high selectivity towards dimers). **1**, **2** and **3** were purified by preparative HPLC and identified by NMR.



1-cyclohexyl-2-phenoxyethanol: ^1H NMR (400 MHz, CDCl_3): δ = 7.36 (t, J = 10 Hz, 2H), 7.03 (t, J = 9.6 Hz, 1H), 6.98 (d, J = 10 Hz, 2H), 4.04 (m, 2H), 3.82 (m, 1H), 1.20-1.80 (m, 11 H). ^{13}C NMR (100.5 MHz, CDCl_3): δ = 159.4, 130.2, 121.8, 115.3, 74.9, 71.0, 41.3, 29.7, 26.8, 26.7.



2-(cyclohexyloxy)-1-phenylethanol: ^1H NMR (400 MHz, CDCl_3): δ = 7.20-7.34 (m, 5H), 4.78 (q, J_1 = 9.2Hz, J_2 = 3.2Hz, 1H), 3.58 (q, J_1 = 9.6Hz, J_2 = 3.2Hz, 1H), 3.34 (t, J = 9.6Hz, 1H), 3.23-3.31 (m, 1H), 1.15-1.90 (m, 10H). ^{13}C NMR (100.5 MHz, CDCl_3): δ = 138.5, 126.5, 125.9, 124.3, 76.3, 71.7, 71.1, 30.4, 23.9, 22.1.



1-cyclohexyl-2-(cyclohexyloxy)ethanol: ^1H NMR (400 MHz, CDCl_3): δ = 3.49 (q, J_1 = 9.2Hz, J_2 = 3.2Hz, 1H), 3.39-3.44 (m, 1H), 3.25 (t, J = 8.8Hz, 1H), 3.16-3.22 (m, 1H), 1.63-1.67 (m, 2H), 1.42-1.62 (m, 17H), 1.20-1.45 (m, 2H). ^{13}C NMR (100.5 MHz, CDCl_3): δ = 78.0, 74.5, 70.2, 40.8, 32.2, 28.8, 26.5, 26.2, 25.8, 24.0.

Table S1. Catalysts screening on the hydrogenolysis reaction of 2-phenoxy-1-phenethanol.

Entry	Catal.	Con./%	Yield/%														
			1 ^a	2	3	4	5	6	7	8	9	10	11	12	13	14	15
1	Ru ^b	>99	0	0	92	0	0	0	0.3	0	0	<0.1	4	0	0.1	0	4
2	Rh	>99	0.04	76	0.5	0	<0.1	<0.1	0.5	0	0	0	10	<0.1	0.5	0	12
3	Pd	23	9	3	0.2	3	<0.1	<0.1	0	0	0	0.4	0.3	0.8	0	6	1
4	Pt	88	33	25	14	2	3	1	0.5	0.5	0.3	<0.1	0.3	0.2	<0.1	<0.1	9
5	Ir	96	46	25	20	0.1	<0.1	0.2	<0.1	0	0	0.5	2	<0.1	<0.1	0.7	2
6	Ag	1	0.3	0.1	0.3	<0.1	<0.1	<0.1	<0.1	0	0	0	0	<0.1	0	0.2	<0.1
7	Au	0.7	0.2	<0.1	<0.1	0.2	0	0	0	0	0	<0.1	0	<0.1	0	0.2	<0.1
8	Cu	6	0.4	0.07	0.00	2	0	0	0	0	0	1	<0.1	0.1	0	2	0.1
9	Fe	4	1	0.5	1	0.2	0.1	<0.1	<0.1	0	0	0	0	<0.1	0	0.2	<0.1
10	Co	87	4.5	0	71	0.1	0.3	0.5	<0.1	0	0	1	0.2	2	0	5	14
11	Ni	58	9	0.9	<0.1	7	0.1	<0.1	0	<0.1	0	15	2	1	0	9	14
12	Re	0.6	0.1	0.2	0	0.1	<0.1	<0.1	<0.1	0	0	0	0	<0.1	0	0.1	0
13	Sn	1	<0.1	<0.1	0	0.5	0	0	0	0	0	0.1	0	<0.1	0	0.4	<0.1
14	NiRu ^c	>99	28	0.8	9	1	1	2	0.3	0.5	0.2	1	16	6	0.6	<0.1	33
15	NiRh	94	26	3	2	6	0.6	0.6	0	0.1	0	15	8	3	<0.1	2	28
16	NiPd	>99	23	1	2	1	0.8	0.6	0	0	0	4	21	7	0.5	<0.1	39
17	NiPt	>99	24	1	2	4	0.7	0	<0.1	0.3	<0.1	10	11	9	0.1	0.4	36
18	NiIr	23	5	0.5	<0.1	2	0	0	0	0	0	6	0.5	0.4	0	5	4
19	NiAg	20	0.4	<0.1	0	0.4	0	0	0	0	0	8	0.4	0.1	0	10	1
20	NiAu	97	18	1	0.6	5	0.4	0.3	0	0.1	0	19	10	4	<0.1	1	37
21	NiCu	17	2	0.00	0	2	0	0	0	0	0	5	0.3	0.3	0	5	2
22	NiFe	36	6	0.00	0	9	0	0	0	0	0	8	1	0.6	0	7	5
23	NiCo	52	10	0.00	0	9	0	0	0	0	0	12	2	1	0	6	12
24	NiRe	34	2	0.3	0.2	7	<0.1	<0.1	0	<0.1	0	9	0.1	1	0	10	5
25	NiSn	2	0.28	0.06	<0.1	0.2	0	0	0	0	0	0.2	0.2	<0.1	0	0.3	0.4

^a The numbers (**1-15**) represent the products showing in Fig. 1a.

^b Reaction conditions: 2-phenoxy-1-phenethanol (0.22 mmol), fresh metal catalysts water solution (0.022 mmol metal, 0.44 mmol PVP, 3mL), 10 bar H₂, 130 °C, 2.5 h.

^c Ni:M ratio is fixed to be 4:1.

Table S2. Hydrogenolysis of 2-phenoxy-1-phenethanol over NiAu catalyst with various Ni:Au ratio.

Entry	Percentage of Au/% ^a	Con./%	Yield/%														
			1	2	3	4	5	6	7	8	9	10	11	12	13	14	15
1	0 ^b	36	5	0.3	<0.1	5	<0.1	<0.1	0	0	0	10	0.6	0.6	0	6	8
2	10	61	12	1	0.3	6	0.1	0.1	0	0	0	15	3	1	<0.1	5	17
3	20	79	15	2	0.4	7	0.2	0.2	<0.1	0	0	20	4	2	<0.1	5	24
4	30	>99	0	0	0	13	<0.1	<0.1	0	0	0	27	0.5	4	0	38	17
5	40	84	13	1	0.2	6	0.2	0.2	0	0	0	22	5	3	<0.1	5	28
6	50	66	11	1	0.2	8	0.2	0.2	0	0	0	17	2	1	0	9	15
7	60	45	8	1	0.1	5	<0.1	<0.1	0	0	0	12	1	0.7	0	8	9
8	70	32	9	1	0.2	5	<0.1	0.1	0	0	0	6	0.4	0.4	0	6	4
9	80	19	4	0.5	<0.1	3	<0.1	<0.1	0	0	0	4	0.2	0.2	0	5	2
10	90	7	0.7	<0.1	<0.1	1	0	0	0	0	0	2	<0.1	0.1	0	3	0.3
11	100	0.7	0.2	<0.1	<0.1	0.2	0	0	0	0	0	<0.1	0	<0.1	0	0.2	<0.1
12	30 ^c	32	7	0.6	<0.1	10	0.1	0.1	<0.1	0	0	5	0.2	0.4	0	7	2

^a The mole fraction of HAuCl₄ used in the synthesis of NiAu catalyst.

^b Reaction conditions: 0.22 mmol 2-phenoxy-1-phenethanol, 3 mL fresh as-prepared metal catalysts water solution containing 0.022 mmol metal catalysts stabilized by 0.44 mmol PVP, 10 bar H₂, 130 °C, 1 h.

^c A physical mixture of fresh Au catalyst solution (0.9 mL) and Ni catalyst solution (2.1 mL) were mixed and used.

Table S3. Hydrogenolysis of 2-phenoxy-1-phenethanol over Ni₇Au₃ catalyst as a function of H₂ pressure.

Entry	P _{H₂} /bar	Con./%	Yield/%														
			1	2	3	4	5	6	7	8	9	10	11	12	13	14	15
1	3	38	3	0.3	0	6	< 0.1	< 0.1	0	0	0	11	0.5	0.6	0	9	7
2	6	53	4	0.3	0	6	< 0.1	< 0.1	0	0	0	17	1	1	0	11	12
3	10	58	7	0.8	0.1	5	0.1	0.1	0	0	0	18	8	1	0	9	16
4	15	35	9	0.6	0.1	5	0.1	< 0.1	0	0	0	8	0.6	0.3	0	6	6
5	20	38	12	1	0.2	3	0.1	< 0.1	0	0	0	9	1	0.4	0	4	8
6	30	42	18	2	0.2	3	0.1	< 0.1	0	0	0	7	1	0.3	0	3	7

Reaction conditions: 2-phenoxy-1-phenethanol (0.22 mmol), freshly prepared Ni₇Au₃ catalysts solution (3 mL, containing 0.022 mmol metal catalysts and 0.44 mmol PVP), H₂, 130 °C, 0.5 h.

Table S4. Kinetics study on the hydrogenolysis of 2-phenoxy-1-phenethanol over Ni and Ni₇Au₃ catalyst.

Entry	Catal.	Time/min	Con./%	Yield/%														
				1	2	3	4	5	6	7	8	9	10	11	12	13	14	15
1	Ni ^a	15	7	2	< 0.1	< 0.1	2	0	< 0.1	0	0	0	1	< 0.1	< 0.1	0	2	0.4
3	Ni	30	19	4	0.2	< 0.1	4	< 0.1	< 0.1	< 0.1	0	0	4	0.1	0.2	0	4	2
4	Ni	50	26	6	0.4	< 0.1	5	< 0.1	< 0.1	< 0.1	0	0	6	0.3	0.2	0	5	4
5	Ni	60	36	5	0.3	< 0.1	5	< 0.1	< 0.1	0	0	0	10	0.6	0.6	0	6	8
6	Ni ₇ Au ₃	10	5	1	0.1	0	0.7	0	0	0	0	0	0.7	< 0.1	< 0.1	0	2	0.6
7	Ni ₇ Au ₃	20	32	6	0.6	< 0.1	4	< 0.1	< 0.1	0	0	0	8	0.5	0.5	0	7	5
8	Ni ₇ Au ₃	30	58	7	0.8	0.1	5	0.1	< 0.1	0	0	0	18	2	1	0	9	16
9	Ni ₇ Au ₃	40	77	10	1	0.2	6	0.2	0.1	0	0	0	23	3	1	< 0.1	7	24
10	Ni ₇ Au ₃	50	84	12	1	0.2	8	0.2	0.2	0	0	0	22	4	2	< 0.1	7	26
11	Ni ₇ Au ₃	60	92	8	0.7	0.07	7	0.2	0.2	0	0	0	28	4	3	< 0.1	8	33
12 ^b	Ni ₇ Au ₃	180	87	7	0.7	< 0.1	7	0.2	< 0.1	< 0.1	0	0	23	3	5	< 0.1	8	34

^a Reaction conditions: 2-phenoxy-1-phenethanol (0.22 mmol), freshly prepared metal catalysts water solution (3 mL, containing 0.022 mmol metal catalysts and 0.44 mmol PVP), 10 bar H₂, 130 °C.

^b With double amount of substrate.

Table S5. Influence of additives (phenol, toluene, cyclohexanol) on the hydrogenolysis of 2-phenoxy-1-phenethanol over Ni and Ni₇Au₃ catalyst.

Entry	Catalyst	Additive	Conv./%	Yield/%														
				1	2	3	4	5	6	7	8	9	10	11	12	13	14	15
1	Ni ^a	None	36	5	0.3	< 0.1	5	< 0.1	< 0.1	0	0	0	10	0.6	0.6	0	6	8
2	Ni	Phenol	21	4	0.5	0.4	7	0.2	0.2	< 0.1	0	0	9	0.1	0.7	0	/	/
3	Ni	Toluene	45	6	0.4	< 0.1	7	0.1	< 0.1	< 0.1	0	0	18	1	1	0	12	14
4	Ni	Cyclohexanol	31	7	0.5	< 0.1	11	0.1	0.1	< 0.1	0	0	14	0.6	1	0	14	/
5	Ni ₇ Au ₃	None	92	8	0.7	0.1	7	0.2	0.2	0	0	0	28	4	3	0	8	33
6	Ni ₇ Au ₃	Phenol	69	10	1	0.1	10	0.2	0.2	< 0.1	0	0	29	3	3	0	/	/
7	Ni ₇ Au ₃	Toluene	60	9	0.8	0.1	6	0.1	0.1	< 0.1	0	0	27	3	3	0	11	26
8	Ni ₇ Au ₃	Cyclohexanol	73	10	0.8	0.1	7	0.2	0.1	< 0.1	0	0	27	3	3	0	11	/

^a Reaction conditions: additive (0.11 mmol), 2-phenoxy-1-phenethanol (0.22 mmol), freshly prepared metal catalysts water solution (3 mL, containing 0.022 mmol metal catalysts and 0.44 mmol PVP), 10 bar H₂, 130 °C, 1 h.

3.4 Determination of the amount of active sites by CS₂ poisoning

In these experiments, all solvents were degassed prior to use and the entire synthesis and poisoning procedure were carried out inside a glove box.

A known amount of CS₂ methanol solution (20 mM) was added into a freshly prepared catalyst aqueous solution (3 mL, 0.022 mmol metal). To exclude any influence of methanol on catalysis, the total methanol added into the catalyst solution was fixed to be 110 μ L, by adding extra, pure methanol. The poisoned catalyst solution and 1-benzyloxy-2-methoxybenzene (0.22 mmol) were sealed in a 20 mL high pressure reactor, took out from the glove box, pressurized with H₂ and heated at 50 °C (a decreased temperature was used to minimize the desorption of CS₂ from Ni or NiAu) under stirring for 2 h (Ni₇Au₃ catalyst) or 4 h (Ni catalyst, as Ni is much less active).

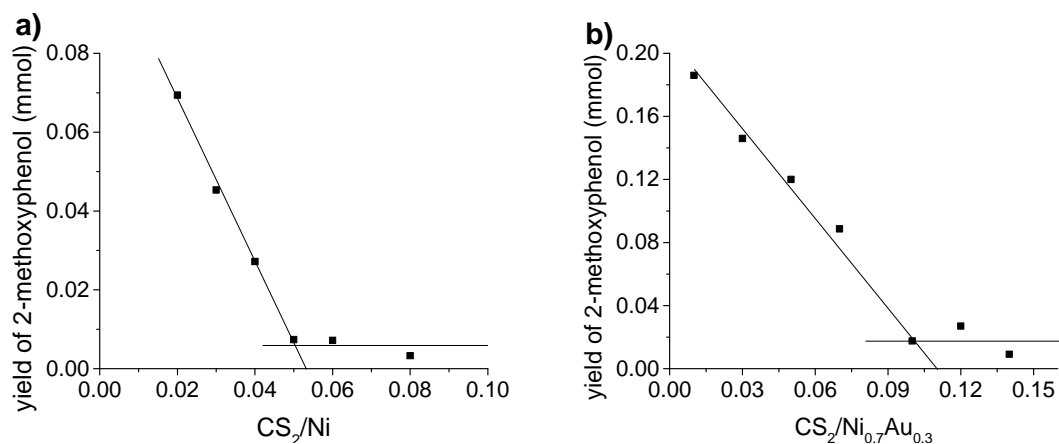


Fig. S1. Yield of 2-methoxyphenol as a function of CS₂/Metal ratio over a) Ni catalysts and b) Ni₇Au₃ catalysts. Reaction conditions: 1-benzyloxy-2-methoxybenzene (0.22 mmol), poisoned Ni or Ni₇Au₃ catalysts water solution (3 mL containing 0.022 mmol metal catalysts, 0.44 mmol PVP, 110 μ L methanol and a certain amount of CS₂), 10 bar H₂, 50 °C, 2 h (Ni₇Au₃) or 4 h (Ni).

From the fitting curves, by assuming one CS₂ molecule blocking two active sites, the active sites fractions of Ni and Ni₇Au₃ catalysts were 10 and 20%, respectively.

Table S6. β -O-4 model compound hydrogenolysis results in literatures.

Entry	Catal.	Temp./°C	P _{H2} /bar	ATOF/h ⁻¹ *	TOF/h ⁻¹	ref
1	Ni ₇ Au ₃	130	10	9	47	In this study
2	Ni/SiO ₂	120	6	1	26	3
3	Ni/AC	200	50	0.3	/	4
4	Cu/ γ -Al ₂ O ₃	150	25	0.4	/	5
5	FeMoP	400	42	14	/	6

* defined as the total number of leaved aryl ether bond divided by the number of all Ni atoms in the catalyst.

4 Catalyst characterization

4.1 Transmission electron microscopy (TEM)

TEM images were taken on a JEOL JEM-2010 microscope operating at 200 kV. To prevent the oxidation of the catalysts, the freshly prepared catalyst solution was passivated by bubbling with CO for 30 minutes immediately after synthesis. TEM samples were prepared by diluting the solution (0.05 ml) with methanol (1.5 ml), following which one drop of the solution was placed on a carbon film covered copper grid and dried under air.

High-resolution TEM (HRTEM), and high-angle annular dark-field scanning TEM (HAADF-STEM) were performed on a FEI Tecnai G² F20 electron microscope operating at 200 kV with a supplied software for automated electron tomography. An energy dispersive X-ray spectroscopy (EDX) analyzer attached to the TEM operating in the scanning transmission electron microscopy (STEM) mode was used to analyze the chemical compositions of nanoparticles, which provides a resolution of 0.7 nm.

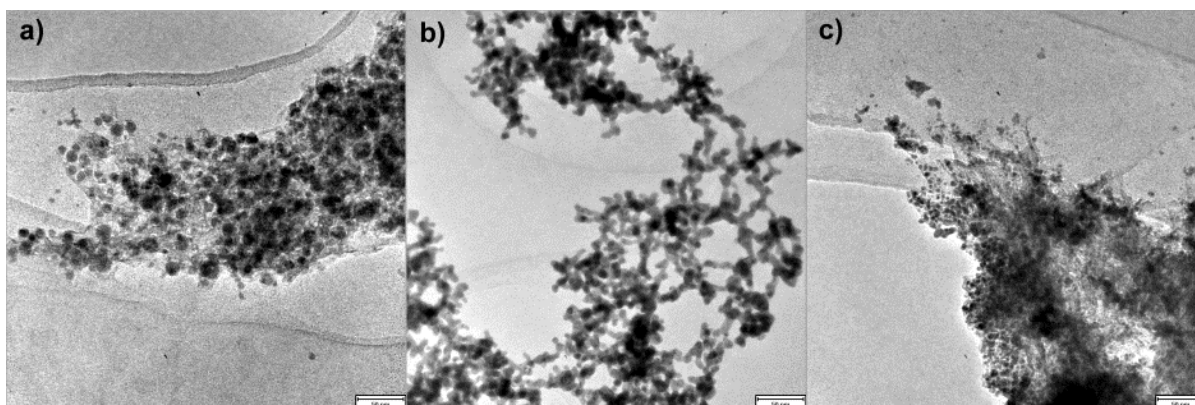
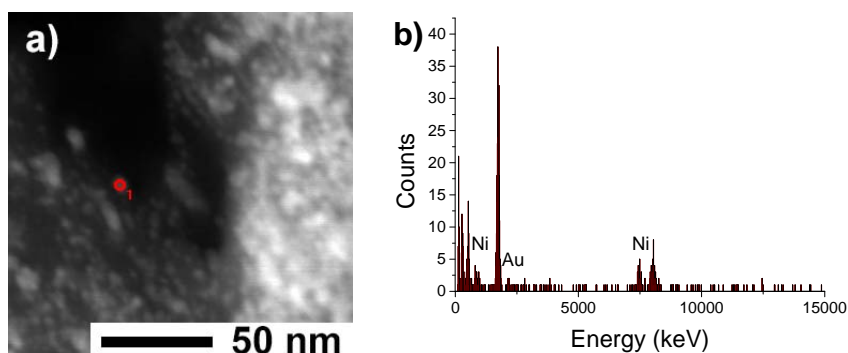


Fig. S2. TEM images of CO passivated a) Ni, b) Au and c) Ni₇Au₃ catalysts. Scale bar: 50 nm



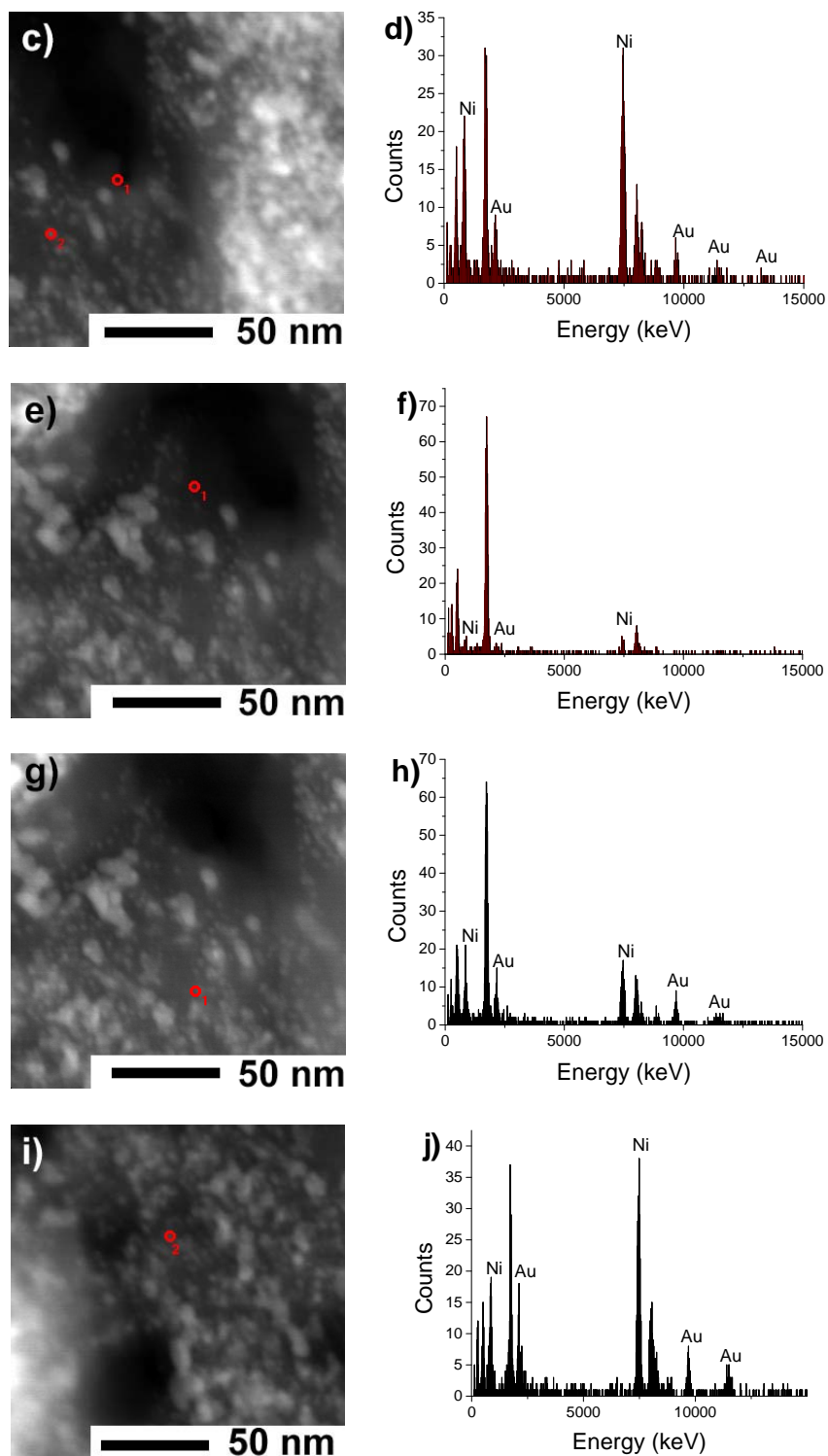


Fig. S3. a-i) HAADF-STEM images of Ni_7Au_3 catalysts with five randomly selected catalyst particles, and b) d) f) h) and j) are the EDX spectra of these selected particles.

4.2 X-Ray powder diffraction (XRD)

XRD was performed on a Bruker D8 Advanced Diffractometer with Cu K α radiation at 40 kV. The XRD sample was prepared by freeze drying the fresh catalyst solution (6 mL) as described in the catalyst preparation section.

4.3 X-ray photoelectron spectroscopy (XPS)

XPS measurements were performed on a VG ESCALAB MKII spectrometer, using mono Al K α X-ray source ($h\nu=1486.71$ eV, 5mA, 15 kV) and calibrating C 1s to 285.0 eV. A thick PVP layer on the catalyst surface would prevent the photoelectrons from the metals to be detected. As such, catalysts for XPS measurement were prepared with reduced PVP (5 instead of 20 equiv.). Fresh catalyst solution (6 ml) was mixed with acetone (50 ml). The mixture was centrifuged and viscous semi-solid material at the bottom of the centrifugation tube was collected, dried under vacuum, and analyzed by XPS. Note that the Au atoms are in the metallic form whereas Ni atoms in the oxide form, due to post-oxidation during sample preparation.

4.4 X-ray absorption (XAS)

Fitting of the NiAu catalyst EXAFS spectra was performed using Artemis software, in conjunction with theoretical scattering paths generated using the *ab initio* program FEFF8.2.^{7, 8} Amplitude scaling factors (S_0^2) for metallic Au and Ni were determined empirically by fitting spectra acquired from the corresponding metal foils; these values were then held fixed in subsequent fits of the NiAu nanoparticle spectra. The spectra were fitted over the ranges indicated in Table 1 using one homometallic (Au-Au or Ni-Ni) and one intermetallic (Au-Ni or Ni-Au) scattering path. Au L₃-edge and Ni K-edge spectra for each AuNi sample were initially fitted separately to obtain reasonable starting values; these values were then used as a starting point for the simultaneous fitting of the Au and Ni spectra. By employing a simultaneous fitting procedure, it was possible to determine a single intermetallic bond length for each sample (via correlation of the Au-Ni and Ni-Au bond distances), thereby providing a more accurate result for this parameter and a more representative fit, overall. Uncertainties were calculated by first sampling shot noise in the 15–25 Å range of the EXAFS spectrum and weighting the resulting off-diagonal elements of the correlation matrix by the square root of the reduced χ^2 value for the fit; thus, experimental noise, goodness-of-fit, and degrees of freedom for each spectrum are all incorporated into the reported final values.⁹

Table S7. Fitting parameters regarding the Fourier-Transformation (FT) and EXAFS fitted regions of Ni₇Au₃ catalyst.

Sample	Edge	FT Region / Å ⁻¹	k-Weight	Fitted Region / Å
Au ₇ Ni ₃	Au L ₃	2.0 - 10.0	2	1.30 - 3.12
	Ni K	2.5 - 13.5	3	1.60 - 2.90

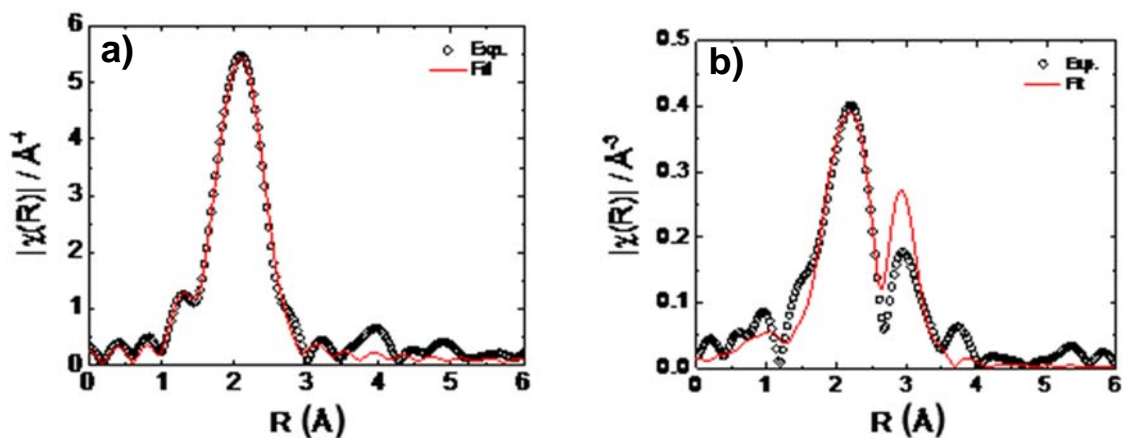


Fig. S4. EXAFS fitting curves for Ni₇Au₃ catalyst at a) Ni K edge and b) Au L_{III} edge.

Table S8. EXAFS fitting results of the Ni₇Au₃ catalyst.

Edge	Path	CN	R/Å	$\sigma^2/\text{Å}^2$	$\Delta E_0/\text{eV}$
Au L _{III}	Au-Au	8(2)	2.79(3)	0.013(5)	-1(2)
	Au-Ni	2(1)	2.59(4) ^a		
Ni K	Ni-Ni	4(1)	2.47(1)	0.012(2)	-8(2)
	Ni-Au	1(1)	2.59(4) ^a		
	Ni-O	4(9)	1.81(6)		

^aAu-Ni and Ni-Au bond distances were correlated during fitting.

4.5 UV-vis spectroscopy

UV-vis spectra were recorded on a Shimadzu 3600 UV-vis spectrophotometer equipped a CPS-240A controller. **For all UV-vis measurements, the concentrations of the metal precursors, reductant and PVP were reduced by a factor of approximately 10, so that the reduced formation rate of the catalyst can be monitored by UV-vis and that the absorption intensity is suitable for UV-vis spectrometer.**

For *in situ* observation of metal reduction, an aqueous solution (2.0 mL) containing PVP (16.5 mM) and metal precursor (0.825 mM, either NiCl₂, HAuCl₄ or a 7:3 combination of the two) was transferred into a standard quartz cell at 16 °C. After addition of a freshly prepared aqueous solution NaBH₄ (8.25 mM, 1.0 mL) maintained at the same temperature (16 °C), and monitored continuously by UV-vis with a time interval of 2 min.

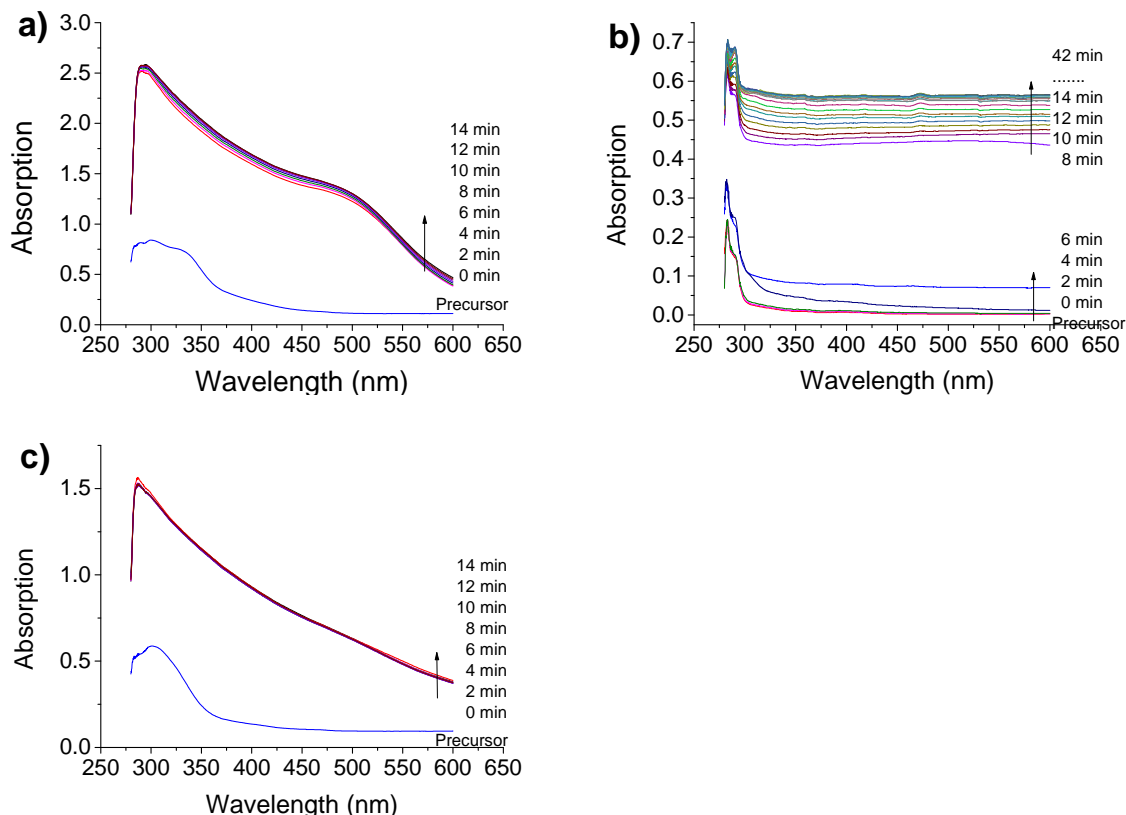


Fig. S5. *In situ* UV-vis monitoring of the formation process of a) Au, b) Ni and c) Ni₇Au₃ catalysts.

4.6 Inductively coupled plasma mass spectrometry (ICP-MS)

To prevent oxidization and leaching of Ni or Au from Ni₇Au₃ into the solution, the Ni₇Au₃ catalyst for ICP-MS analysis was prepared in a glove box. Then Ni₇Au₃ catalyst solution (3 mL) was transferred to an Amicon® ultra centrifugal filter (ultracel-3K) in the glove box, and then took out and centrifuged at 8000 rpm for 30 minutes. To wash the catalyst, the tube was transferred back into the glove box and added 5 mL degased water, and then taken out of the glove box and centrifuged at 8000 rpm for 30 minutes. After repeating the procedure 3 times, aqua regia (6 mL) was added to the tube to dissolve the catalyst on the filter. The mixture was refluxed for 2 hours, and diluted with deionized water to 100.0 mL. ICP-MS was recorded on Leeman ICP-MS system.

4.7 DFT calculation

Calculations were performed using periodic density functional theory with the revised Perdew-Burke-Ernzerhoff-Van der Waals functional (DFT-RPBE-VdW),¹⁰ and using the projector-augmented wave (PAW) method as implemented in VASP¹¹⁻¹⁴ and with a kinetic energy cutoff of 400 eV.

The surface was modeled as a 3-layer, p(4x4) (111) unit cell where the bottom layer was fixed at the optimized Ni lattice of 3.57 Å. Repeated slabs were separated by at least 10 Å vacuum. The NiAu catalyst

slab has a 3:1 Ni:Au ratio in the top layer and only Ni in the second and third layer. The Brillouin zone was sampled using a (3x3x1) Monkhorst Pack k-point grid.¹⁵

Initial guesses for the transition states were obtained with the nudged elastic band (NEB) method as implemented in VASP and fully optimized.¹⁶ The transition states were confirmed to be first order saddle points using frequency calculations. As reaction barrier, the energy difference between the transition and $\text{XO}^* + \text{H}^*$ in two different calculations state is taken. This corresponds to the reaction barrier at a low coverage surface.

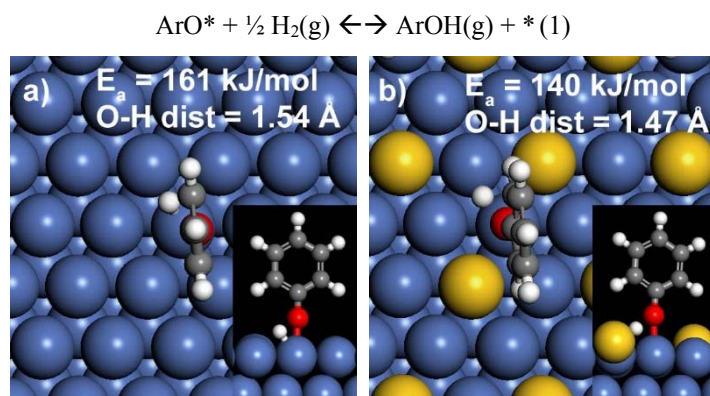


Fig. S6. Transition states and activation barriers for the hydrogenation of ArO^* intermediates on Ni(111) and on $\text{Ni}_3\text{Au}(111)$. Au reduces the calculated activation barrier by 21 kJ/mol.

ArO^* adsorbs upright at the hcp hollow site of Ni(111) (Fig. 3a) and is quite stable with a reaction energy of +42 kJ/mol for reaction (1) (Table S9). The stability of a planar ArO^* species on Ni(111) is comparable. The presence of 0.25 ML Au significantly destabilizes the phenoxy species by 50 kJ/mol at hollow sites containing a Au atom and by 37 kJ/mol at Ni hollow sites (Table S9). The Ni-O distance at the Ni sites increases marginally from 2.00 Å on Ni(111) to 2.02 Å on NiAu. At hollow sites containing a Au atom, phenoxy moves to a Ni bridge site. In agreement with the reduced stability, the presence of Au significantly decreases the ArO^* hydrogenation barrier.

Table S9: Relative energies for the overall reaction $\text{XO}^* + \frac{1}{2} \text{H}_2(\text{g}) \rightarrow \text{XOH} + *$ on Ni and NiAu in kJ/mol, as well as the O-H distance of the forming bond in the TS in Å.

	X = H		X = Ar	
	Ni	NiAu	Ni	NiAu
$\text{XO}^* + \frac{1}{2} \text{H}_2(\text{g}) \rightarrow \text{XOH}(\text{g})$	-5	-55	40	5
$\frac{1}{2} \text{H}_2 + * \rightarrow \text{H}^*$	-35	-20	-35	-20
$\text{XO}^* + \text{H}^* (\text{inf. far apart}) \rightarrow \text{TS}$	130	110	160	140
Forming O-H distance (Å)	1.55	1.60	1.54	1.47

5 Conversion of other lignin model compounds and organosolve lignin

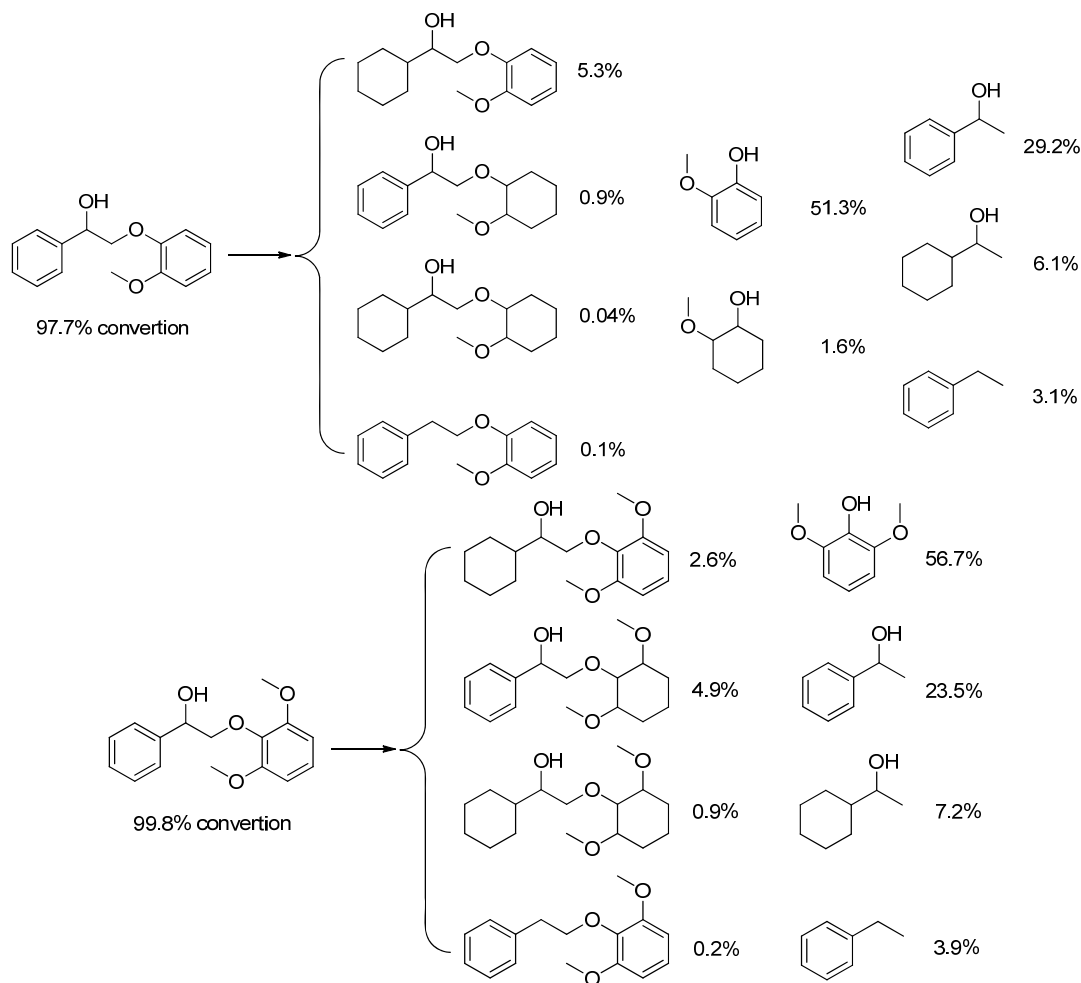


Fig. S7. Hydrogenolysis of 2-(2-methoxyphenyl)oxy-1-phenethanol and 2-(2,6-dimethoxyphenyl)oxy-1-phenethanol. Reaction condition: substrate (0.22 mmol), freshly prepared Ni₇Au₃ catalyst water solution (3 mL, containing 0.022 mmol metal catalysts and 0.44 mmol PVP), 10 bar H₂, 130 °C, 1h.

Table S10. Hydrogenolysis of 1-benzyloxy-2-methoxybenzene over Ni and Ni₇Au₃ catalyst. Reaction conditions: 1-benzyloxy-2-methoxybenzene (0.22 mmol), freshly prepared metal catalyst water solution (3 mL, containing 0.022 mmol metal catalysts and 0.44 mmol PVP), 10 bar H₂, 130 °C, 0.5 h.

Entry	T/°C	Catalyst	Conversion/%	Yield/%	
				Toluene	Guaiacol
1	130	Ni	72	14	33
2	130	Ni ₇ Au ₃	96	14	44
3	60	Ni	5	1	4
4	60	Ni ₇ Au ₃	20	4	7

Table S11. Hydrogenolysis of diphenyl ether over Ni₇Au₃ catalyst. Reaction conditions: diphenyl ether (0.22 mmol), freshly prepared Ni₇Au₃ catalyst water solution (3 mL, containing 0.022 mmol Ni₇Au₃ catalysts and 0.44 mmol PVP), 10 bar H₂, 130 °C.

Entry	T/°C	Time/h	Conversion/%	Yield/%			
				Phenol	Cyclohexanol	Benzene	Cyclohexane
1	130	1	5	0.6	3	1	0.1
2	150	1	12	0.8	5	1	0.1
3	130	12	50	0.8	18	2	0.1

5.1 Conversion of organosolv lignin

Organosolv lignin (50 mg), freshly prepared Ni₇Au₃ catalyst (0.022 mmol in 3 mL water) and magnetic stirrer were charged into a high pressure reactor (20 mL). After flushing with H₂ three times, the reactor was charged with 10 bar H₂, and put into a preheated oil bath with a stirring speed of 1000 rpm. After the reaction, the reactor was quenched to ambient temperature using cooling water. The reaction mixture was extracted with chloroform (3×20 mL), and then the combined chloroform phase was dried in vacuum to give the product as a brown solid. The solid was dissolved in DMSO-d₆ and DMF to run NMR and GPC analysis, respectively.

5.2 Gel permeation chromatography (GPC)

GPC analysis was carried out with a system equipped with a Waters 2410 refractive index detector, a Waters 515 HPLC pump and two Waters styragel columns (HT 3 and HT 4) using DMF as eluent at a flow rate of 1 ml/min at 25 °C. The raw data were processed using narrow polystyrenes as calibrations on software Breeze.

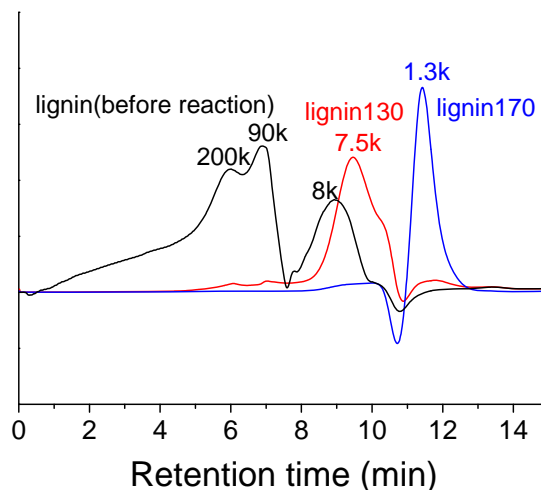


Fig. S8. GPC spectra of Organosolv lignin, **lignin130** and **lignin170**.

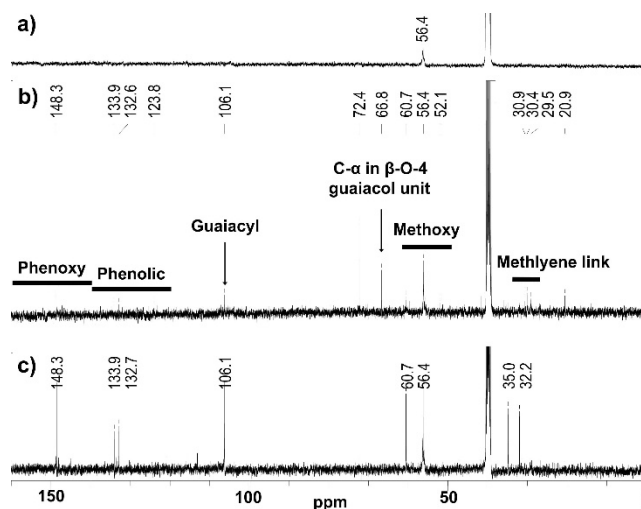


Fig. S9. ^{13}C -NMR spectra of a) organosolv lignin, b) products after depolymerization over Ni_7Au_3 at $130\text{ }^\circ\text{C}$ and 1 hour (**lignin130**) and c) products after depolymerization at $170\text{ }^\circ\text{C}$ and 12 hours (**lignin170**).

References:

1. J. M. Pepper and M. Siddiqueullah, *Can. J. Chem.*, 1961, **39**, 1454-1461.
2. J. M. Nichols, L. M. Bishop, R. G. Bergman and J. A. Ellman, *J. Am. Chem. Soc.*, 2010, **132**, 12554-12555.
3. J. He, C. Zhao and J. A. Lercher, *J. Am. Chem. Soc.*, 2012, **134**, 20768-20775.
4. Q. Song, F. Wang and J. Xu, *Chem. Commun.*, 2012, **48**, 7019-7021.
5. Z. Strassberger, A. H. Alberts, M. J. Louwse, S. Tanase and G. Rothenberg, *Green Chem.*, 2013, **15**, 768-774.
6. D. J. Rensel, S. Rouvimov, M. E. Gin and J. C. Hicks, *J. Catal.*, 2013, **305**, 256-263.
7. M. Newville, *J. Synchrotron. Radiat.*, 2001, **8**, 322-324.
8. B. Ravel and M. Newville, *J. Synchrotron. Radiat.*, 2005, **12**, 537-541.
9. M. Newville, B. I. Boyanov and D. E. Sayers, *J. Synchrotron. Radiat.*, 1999, **6**, 264-265.
10. J. Klimeš, D. R. Bowler and A. Michaelides, *Phy. Rev. B*, 2011, **83**, 195131.
11. P. E. Blöchl, *Phy. Rev. B*, 1994, **50**, 17953-17979.
12. G. Kresse and D. Joubert, *Phy. Rev. B*, 1999, **59**, 1758-1775.
13. G. Kresse and J. Hafner, *Phy. Rev. B*, 1994, **49**, 14251-14269.
14. G. Kresse and J. Furthmüller, *Comput. Mater. Sci.*, 1996, **6**, 15-50.
15. H. J. Monkhorst and J. D. Pack, *Phy. Rev. B*, 1976, **13**, 5188-5192.
16. G. Henkelman and H. Jonsson, *J. Chem. Phys.*, 2000, **113**, 9978-9985.